Remote Sensing of Environment 207 (2018) 42–49

Contents lists available at ScienceDirect

Remote Sensing of Environment

journal homepage: www.elsevier.com/locate/rse

The effects of global positioning system receiver accuracy on airborne laser scanning-assisted estimates of aboveground biomass

Ronald E. McRoberts[a,*], Qi Chen[b], Brian F. Walters[a], Daniel J. Kaisershot[a]

[a] Northern Research Station, U.S. Forest Service, Saint Paul, MN, USA
[b] Department of Geography, University of Hawai'i at Mānoa, Honolulu, Hawai'i, USA

ARTICLE INFO

Keywords:
Model-assisted estimator
Forest inventory

ABSTRACT

National forest inventories routinely report estimates of parameters related to aboveground biomass (AGB), but sample sizes are often insufficient to satisfy precision guidelines and reporting requirements. Aerial photography, satellite imagery, and increasingly airborne laser scanning (ALS) data are all used as sources of auxiliary information to address this challenge.

Combining inventory ground plot and ALS data requires that the data be co-registered to a common coordinate system. When measuring plots, inventory field crews typically obtain estimates of plot coordinates using global positioning system (GPS) receivers of varying degrees of accuracy. GPS-related errors in plot coordinates contribute to a sequence of adverse effects: (i) plot data are associated with erroneous ALS metrics, (ii) statistical models fit to such data may not adequately represent the true relationship between the plot data and the ALS metrics; and (iii) bias may be induced into model-assisted statistical estimators of population parameters.

The primary objectives of the study focused on assessing the effects of GPS receiver inaccuracies on the estimated bias and precision of model-assisted estimators of mean AGB per unit area. The underlying motivation was to determine if the advantages of using ALS data as auxiliary information can be achieved apart from the substantial additional expense of purchasing GPS receivers with sub-meter accuracy. The analyses focused on comparing estimates based on three variations of plot coordinates obtained using field crew GPS receivers with maximum location errors on the order of 5–10 m to estimates based on plot coordinates obtained using survey grade GPS receivers with sub-meter accuracy. The study area was in north central Minnesota in the USA and is characterized by both upland and lowland forest areas interspersed with lakes and wetlands. The primary results were twofold. First, estimates of mean AGB per unit area based on plot coordinates obtained using the less accurate field crew GPS receivers varied little from estimates based on the much more accurate survey grade receivers. Second, standard errors were greater by as much as 20% when using field crew GPS receivers than when using survey grade GPS receivers. However, even though the ALS-assisted standard errors obtained using field crew GPS receivers were greater than when using survey grade receivers, they were still substantially smaller than satellite image-assisted standard errors. Thus, the operational conclusion is that avoiding the substantial additional cost of providing a survey grade GPS receiver for each of more than 100 field crews likely outweighs the adverse consequences of somewhat larger standard errors.

1. Introduction

National forest inventories (NFI) routinely report estimates of parameters related to aboveground biomass and growing stock volume on which it is based. The estimates are used for multiple purposes including strategic planning (USDA-FS, 2012), national reporting, and reporting for an increasing number of international agreements such as the Global Forest Resources Assessment (FAO, 2016) and Annex 1 of the United Nations Framework Convention on Climate Change (UNFCCC, 2006). However, for important inventory parameters, particularly those related to aboveground biomass and growing stock volume, NFI sample sizes are often not large enough to produce precision that satisfies guidelines and reporting requirements. Remotely sensed data are increasingly used as a source of auxiliary information to address this challenge.

From as early as the 1950s, aerial photography was used with double sampling for stratification to increase the precision of inventory estimators (Bickford, 1952; Poso, 1972; Poso and Kujala, 1978). In

* Corresponding author.
E-mail address: rmcroberts@fs.fed.us (R.E. McRoberts).

https://doi.org/10.1016/j.rse.2017.09.036
Received 2 March 2017; Received in revised form 25 September 2017; Accepted 28 September 2017
0034-4257/ Published by Elsevier Inc.

recent years, satellite imagery has replaced aerial photography as a source of information for constructing strata in many countries (McRoberts et al., 2002, 2006; Nilsson et al., 2005). With the latter approaches, the satellite imagery is often classified with respect to selected forest attributes, and the classes or aggregations of the classes serve as strata for stratified estimation (Miles et al., 2011, p. 62). More recently, metrics derived from distributions of airborne laser scanning (ALS) height data have been shown to be excellent predictors of forest attributes such as growing stock volume and biomass. The resulting spatial products depicting the model predictions have then been used to increase the precision of estimators of inventory parameters, often to an even greater degree than satellite spectral data (Næsset et al., 2011; McRoberts et al., 2012, 2013; Steinmann et al., 2013; Saarela et al., 2015).

Multiple recent studies have documented the utility of combining NFI or NFI-like field plot data and ALS data with small pulse densities. In 2002 and 2004, Austria acquired nationwide ALS data with densities of 1–4 pulses/m^2 to construct a DTM. Hollaus et al. (2009) combined these ALS data with NFI data to construct volume models with $R^2 = 0.79$. Between 2009 and 2015, Sweden acquired nationwide ALS data with densities of 0.5–1.0 pulses/m^2 for construction of a DTM. Nilsson et al. (2017) combined these ALS data with NFI data obtained from 300-m^2 plots and constructed volume models that produced relative RMSEs of 20–25%. In the United States of America (USA), ALS data, mostly for constructing DTMs, have been acquired for most of the eastern half of the country. For study areas in Minnesota, Chen et al. (2016) and McRoberts et al. (2016, 2017) combined these ALS data with densities of approximately 0.67 pulses/m^2 with NFI data and constructed biomass-ALS models with pseudo-R^2 as great as 0.80. These studies have multiple features in common: (i) large study areas; (ii) ALS data with small pulse densities acquired for the primary purpose of constructing DTMs; (iii) NFI or NFI-like ground plot data; and (iv) models for predicting forest volume or biomass using ALS metrics as independent variables. However, only Chen et al. (2016) and McRoberts et al. (2016, 2017) extended the analyses from model construction to assessment of the utility of the ALS data for inferences for population parameters. A crucial finding of the latter studies was that use of ALS data as auxiliary information decreased the variances of estimators of AGB-related parameters by factors as great as 3.5.

An assumption underlying use of ALS metrics based on distributions of pulse return heights as model independent variables is that the number of pulse returns per plot is sufficiently large that the height distributions are adequately characterized and that metrics derived from the distributions are reliably estimated (Magnussen and Boudewyn, 1998). Of importance, it is the number of pulses per plot that is crucial, not just the plot size or the pulse density individually. Vauhkonen et al. (2014) reported that numbers of pulses per plot as small as 50 may have no adverse effects on the quality of fit of volume or biomass models.

Combining ground plot and ALS data requires that the data be co-registered to a common coordinate system. Coordinates for inventory ground plots are typically acquired by field crews using global positioning system (GPS) receivers whose maximum location errors may be as small as sub-meter but also may be as great as 5–10 m. A crucial effect of GPS errors is that the area of the ground plot does not correspond exactly with the ground area for which the ALS metrics are calculated. As the ratio of GPS error to plot radius increases from 0 to 2, the common area of the plot and the circular area for which the ALS metrics are calculated decreases nearly linearly from 100% to 0%. For statistical modelling purposes, this condition violates the regression assumption that independent variables are observed without error and is characterized as *errors-in-variables*. An effect of errors in variables is that estimated models, regardless of the qualities of fit of the models to the data, may not adequately represent the relationships between the dependent variable and the independent variables when the latter are observed without error. If so, bias is induced into population parameter estimators that rely on the model predictions. For simple linear models, independent random errors in the independent variable cause the estimate of the slope to tend to zero, an effect characterized as *regression dilution* or *regression attenuation*. For nonlinear models and non-parametric prediction techniques such as Random Forest and k-Nearest Neighbors, the effects are difficult to generalize and must be assessed on a case-by-case basis.

The adverse consequences of plot positional errors were confirmed by Gobakken and Næsset (2009) and Mauro et al. (2011) who assessed the effects on ALS metrics, by Frazer et al. (2011) who assessed the effects on lidar-based model predictions, and by Saarela et al. (2016) who assessed the effects on estimated bias of large area ALS-assisted estimators. Although the results of these studies are not entirely comparable, in general the effects of positioning errors were minimal when plot radii were 10 m or greater and maximum positioning errors were less than 5 m.

An important operational issue for NFIs is the degree to which use of GPS receivers with maximum errors on the order of 5–10 m adversely affects the utility of ALS data for enhancing forest inventory inferences. If a large portion of the potential utility of ALS data for enhancing forest inventory inferences can be realized using GPS receivers with maximum errors on the order of 5–10 m, then considerable cost savings may be possible; if not, substantial expense may be necessary to provide large numbers of field crews with GPS receivers with sub-meter accuracies. Thus, the primary objective of the study was to assess the effects of errors-in-variables induced by GPS location error on estimated bias and precision of model-assisted estimators of mean aboveground biomass per unit area (AGB, Mg/ha) using ALS data with small pulse densities as auxiliary information. A secondary objective was to investigate a possibility for mitigating the effects of errors-in-variables. Assessments were based on comparisons of estimates based on ALS metrics corresponding to locations obtained using GPS receivers with maximum location errors of 5–10 m to estimates based on ALS metrics corresponding to locations obtained using GPS receivers with sub-meter accuracy. Although pseudo-R^2 was used to compare the accuracies of predictions for models of relationships between AGB and ALS metrics, the primary assessment criteria were inferences expressed by estimates of population means and their standard errors for AGB obtained using model-assisted estimators.

2. Data

2.1. Study area

The 7583-km^2 study area consisted of the entirety of Itasca County in north central Minnesota in the USA (Fig. 1) and is characterized topographically by low plains, rolling hills, wetlands and water with elevations ranging from 113 to 164 m above sea level. Land cover includes approximately 80% forest land consisting of uplands with mixtures of pines (*Pinus* spp.) spruce (*Picea* spp.) and balsam fir (*Abies balsamea* (L.) Mill.) and lowlands with spruce (*Picea* spp.), tamarack (*Larix laricina* (Du Roi) K. Koch), white cedar (*Thuja occidentalis* (L.)), and black ash (*Fraxinus nigra* Marsh.).

2.2. Forest inventory data

Data were obtained for plots established by the Forest Inventory and Analysis (FIA) program of the U.S. Forest Service which conducts the NFI of the USA. The FIA program has established field plot centers in permanent locations using a systematic unaligned sampling design that is regarded as producing an equal probability sample (McRoberts et al., 2010). Each FIA plot consists of four 7.32-m (24-ft) radius circular subplots that are configured as a central subplot and three peripheral subplots with centers located at 36.58 m (120 ft) and azimuths of 0°, 120°, and 240° from the center of the central subplot. Field crews observe species and measure diameter at breast-height (dbh, 1.37 m,

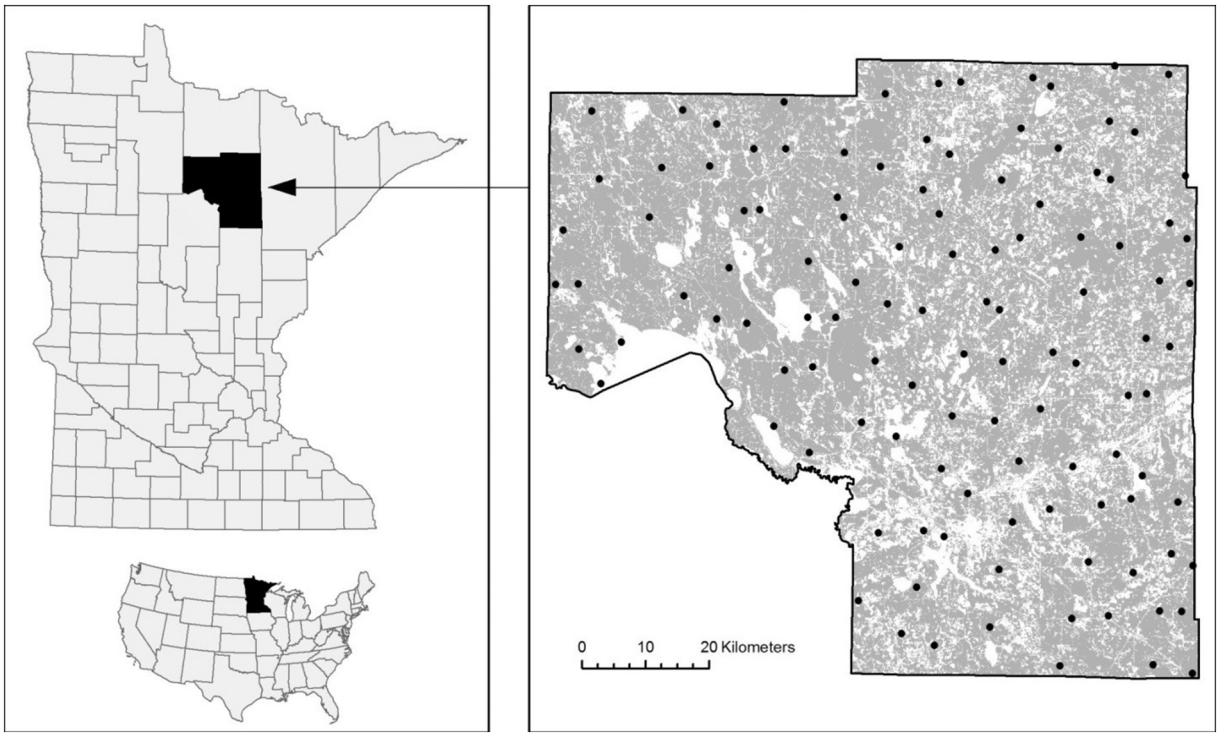

Fig. 1. Study area in Itasca County, Minnesota, USA.

Table 1
GPS receiver attributes.

Attribute	GPS receiver		
	Field crew	Survey	
Vendor	Emtac	Trimble	Trimble
Model	Mini S3	Geo 7x	Geo Explorer 6000
Channels	20	220	220
Dimensions	3D	3D	3D
Acquisitions	60	180	60
Antenna	Internal	External	External
Post-processing	No	Yes	Yes

4.5 ft) and height for all trees with dbh of at least 12.7 cm (5 in) on each 7.32-m radius subplot and for all trees with dbh of at least 2.54 cm (1 in) on 2.07-m (6.8-ft)-radius microplots with centers at subplot centers. Allometric model predictions of individual tree aboveground biomass are aggregated at plot-level and scaled to a per unit area basis. For this study, uncertainty associated with the allometric model predictions of individual tree stem biomass was ignored. Subplot-level AGB for trees with dbh of at least 12.7 cm was estimated, scaled to a per unit area basis, designated *AGB5*, and associated with ALS metrics for the entire subplot. Subplot-level AGB for trees with dbh of at least 2.54 cm but less than 12.70 cm was also estimated, scaled to a per unit area basis, added to AGB5 to obtain *AGB1*, and associated with ALS metrics for the entire plot. Thus, apart from plot location error, AGB5 corresponds exactly with the ALS metrics, whereas AGB1 corresponds somewhat inexactly because the small tree component of AGB1 is based on an area that is smaller than the area on which the ALS metrics are based. However, this use of smaller concentric circular plots for smaller trees is characteristic of most NFIs.

Data were used for only the central subplots of the 242 plots measured in 2014 and 2015, because these were the only subplots and years for which plots coordinates were obtained using survey grade GPS receivers with sub-meter accuracy. The large correlations among observations for subplots of the same plot mean that little information is lost by considering only the central subplot. In addition, preliminary analyses indicated that residual variation around model predictions was less when using only the central subplot than when using all four subplots separately and their associated ALS metrics or when using data aggregated for all four subplots and ALS metrics corresponding to a circle circumscribing the four subplots.

2.3. Plot coordinates

Four sets of plot coordinates were used for the study. First, coordinates of centers of plots measured in 2014 and 2015 were estimated using survey grade GPS receivers with sub-meter accuracy and were designated *survey* coordinates. Second, each time an FIA plot is measured, field crews independently estimate the coordinates of the centers of forested, partially forested, or previously forested plots using GPS receivers for which maximum location errors are generally less than 5 m but may be as large as 10 m (Table 1). For future reference, the plot coordinates most recently estimated using the latter GPS receivers are designated *field crew* coordinates.

Because the combination of 7.32-m radius plots and maximum positioning errors of 5 m are not within the intervals for which the effects of positioning errors have been reported to be negligible (Gobakken and Næsset, 2009; Mauro et al., 2011; Frazer et al., 2011), two additional sets of plot coordinates were considered. Between 1999 and 2015, plots in the study area were measured every five years with the result that most plots were measured at least three times. An underlying question is whether the means over multiple independently obtained *field crew* coordinates converge to the *survey* coordinates; if so, means of field crew coordinates may ameliorate or even circumvent the adverse effects on estimated bias and precision of errors-in-variables induced by GPS location error. Thus, the third approach to estimating plot coordinates entailed calculating the mean of the *field crew* coordinates for each plot over all measurements. These means over multiple *field crew* coordinates were designated *mean field crew* coordinates. The fourth approach is based on the premise that one or more individual sets of *field crew* coordinates may be seriously in error. For all plots with three or more sets of *field crew* coordinates, the deviations between the

individual sets of *field crew* coordinates and their respective means were calculated. If the common area between a 7.32-m radius circle with center at the *mean field crew* coordinates and a similar circle with center at coordinates with the maximum deviation from the mean was proportionally less than 0.25, those *field crew* coordinates were removed from consideration, and the *mean field crew* coordinates were recalculated. The resulting coordinates based on the recalculated means were designated *adjusted mean field crew* coordinates. For a variety of reasons including establishment of new plots, inability to measure a small number of existing plots, and missing data, a small number of plots had only one or two sets of *field crew* coordinates. For these plots, no such analysis was possible and the *mean field crew coordinates* were used.

2.4. Airborne laser scanning data

Wall-to-wall ALS data were acquired in April 2012 with a nominal pulse density of 0.67 pulses/m^2. Ground returns were classified by the provider and were used to construct a digital terrain model via interpolation using the Tiffs (Toolbox for Lidar Data Filtering and Forest Studies) software (Chen, 2007). Multiple factors affect the validity of the assumption that the number of pulses per plot is sufficient to characterize plot-level distributions of pulse return heights. First, minimum ALS height thresholds in the range of 1.0–2.0 m are often used to discriminate between pulses returned from trees and pulses returned from non-tree ground vegetation (Næsset et al., 2011; Saarela et al., 2015; Chirici et al., 2016; Hopkinson et al., 2016). Greater thresholds reduce the number of returns per plot and thereby exacerbate the adverse effects of small plots and small pulse densities. Second, for analysis purposes, ALS data are often restricted to first or only pulse returns rather than all returns (Saarela et al., 2015; Babcock et al., 2015; Cao et al., 2016). This practice also reduces the number of pulses per plot and similarly exacerbates the same adverse effects. Therefore, for this study that uses relatively small plots and ALS data characterized by small pulse densities, all pulse returns from all heights were used.

Distributions of all pulse return heights were constructed for the 168.3-m^2 plots using each of the four sets of plot coordinates (*survey*, *field crew*, *mean field crew*, *adjusted mean field crew*). Distributions were also constructed for 169-m^2 square cells that tessellated the study area and served as population units. ALS metrics for each plot and cell included the mean (h_{mn}), standard deviation (h_{sd}), skewness (h_{sk}), kurtosis (h_{ku}), and quadratic mean height (h_{qm}) of the distributions of heights for all pulse returns (Lefsky et al., 1999; Chen et al., 2012). In addition, heights corresponding to the 10th, 20th, …, 100th percentiles (h_{10}, h_{20}, …, h_{100}) of the distributions were calculated as were canopy densities expressed as the proportions of pulse returns with heights greater than 10%, …, 90%, 95% (d_{10}, …, d_{90}, d_{95}) of the range between a minimum ALS above ground height threshold and the 95th height percentile (Gobakken and Næsset, 2008).

3. Methods

3.1. Data outliers

The objective focused on estimating the effects of GPS location error on inferences, particularly means and SEs. To isolate the effects of this source of uncertainty, other sources whose effects are confounded with them must be identified and eliminated. In this regard two sources of confounded uncertainty related to plot-level AGB observations were addressed.

First, because the ALS data were acquired in 2012 but the plots were not measured until 2014 and 2015, some plots were harvested or otherwise substantially disturbed between the two dates. To alleviate this discrepancy, plots were deleted from further analyses if they satisfied three criteria: (i) 2009 or 2010 AGB greater than the 20th percentile of distribution of observed AGB for forest plots, (ii) AGB = 0 for 2014 or 2015, and (iii) h_{qm} greater than the 20th percentile of the distribution of observed h_{qm} for plots satisfying the first two criteria. To evaluate the effects of GPS location error on the latter criterion, two subordinate investigations were conducted; for the first, the h_{qm} criterion was eliminated from consideration, and for the second, plot-level h_{qm} was replaced with mean h_{qm} for a 3 × 3 block of cells centered on the plot location. Second, the FIA program classifies plots with respect to forest use, not forest cover. Therefore, plots with substantial tree-based AGB but classified as non-forest use (e.g., orchards, parkland, residential property) would not be measured in the field and would have AGB = 0 recorded. To alleviate this discrepancy, plots were deleted from further analyses if they satisfied two criteria: (i) AGB = 0 for 2014 or 2015, and (ii) h_{qm} greater than the 20th percentile of the distribution of observed h_{qm}. Because GPS receivers were not used to obtain coordinates of centers for non-forest plots, no subordinate analyses were conducted for this factor. Selection of the 20th percentile for both factors is arbitrary, albeit conservative because it leads to fewer deletions than smaller percentiles. In addition, distributions of observed h_{qm}, and therefore deletions, are affected by the particular set of plot coordinates used.

3.2. Model

A basic model of the relationship between AGB1 and AGB5 as dependent variables and the ALS metrics as independent variables was formulated as,

$$y_i = \beta_0 \cdot x_i^{\beta_1} + \varepsilon_i, \tag{1}$$

where i indexes plots, y_i is either AGB1 or AGB5, x_i is an ALS metric, ε_i is a random residual, and the βs are parameters to be estimated. An advantage of this model is that when the ALS metrics are zero, as is the case for many non-forest plots, the prediction will also be zero. Preliminary analyses indicated that h_{qm} was the individual ALS metric that produced the most accurate predictions. This result has been independently confirmed by Nelson et al. (2009), Boudreau et al. (2008), Chen et al. (2012), and Chen et al. (2015). All possible combinations of one, two, and three additional independent variables beyond h_{qm} were considered for inclusion into a modification of the model, but none contributed to statistically significantly improving the quality of fit of the model to the data.

As with most biological data, residual heteroscedasticity in the form of greater residual variances for larger observations was evident. Although the mathematical form of Eq. (1) readily lends itself to a log-log transformation for purposes of either linearization or reduction of heteroscedasticity, weighted nonlinear least squares were used for these analyses. The heterogeneous model residual variance, σ_i^2, was characterized using a 5-step procedure (McRoberts et al., 2016, Section 3.2.2): (i) calculate the model prediction residuals as $\varepsilon_i = y_i - \hat{y}$ where $\hat{y}_i = \hat{\beta}_1 \cdot x_i^{\hat{\beta}_2}$; (ii) order the pairs ($x_i$, ε_i) with respect to x_i; (iii) aggregate the ordered pairs into groups of size 5 or more; (iv) for each group, g, calculate the mean, $\overline{x}_g$, of the predictor variable and the standard deviation, $\hat{\sigma}_g$, of the grouped residuals; and (v) model the relationship between $\hat{\sigma}_g$ and $\overline{x}_g$ as,

$$\hat{\sigma}_g = \lambda \cdot \overline{x}_g + \varepsilon_g, \tag{2}$$

where λ is a model parameter estimated using ordinary least squares techniques. Each observation was weighted inversely to its residual variance estimated by substituting h_{qm} for $\overline{x}_g$ in Eq. (2).

Residuals analysis included calculating standardized residuals as ratios of ε_i and $\hat{\sigma}_i$. Plot-level observations with standardized residuals greater than 3.5, a very conservative criterion, were deleted, and the model was refit to the data. F-tests based on the extra sum of squares principle were used to assess whether inclusion of additional independent variables contributed to statistically significantly improving the quality of fit of the models to the data (Draper and Smith, 1981,

Section 2.7). Fits of the model to the data were characterized using pseudo-R^2,

$$R^{2*} = \frac{SS_{mn} - SS_{res}}{SS_{mn}}, \tag{3}$$

where SS_{mn} is the sum of squared differences between AGB observations and their mean, and SS_{res} is the sum of squared residual differences between AGB observations and their corresponding model predictions.

3.3. Inference

For forest inventory purposes, the ultimate analytical objective is a statistical inference in the form of a confidence interval calculated as $\hat{\mu} \pm t \cdot \sqrt{V\hat{a}r(\hat{\mu})}$ where $\hat{\mu}$ is the estimate of a population mean, $V\hat{a}r(\hat{\mu})$ is an estimate of the variance of the estimator of the mean, and t corresponds to the confidence level. Thus, analytical components of the study focused on $\hat{\mu}$ and its standard error, $SE(\hat{\mu}) = \sqrt{V\hat{a}r(\hat{\mu})}$.

3.3.1. Simple random sampling estimators

With equal probability sampling designs, the simplest approach to inference is to use the familiar *simple random sampling* (*SRS*) estimators for means and their variances,

$$\hat{\mu}_{SRS} = \frac{1}{n}\sum_{i=1}^{n} y_i \tag{4a}$$

and

$$V\hat{a}r(\hat{\mu}_{SRS}) = \frac{\sum_{i=1}^{n}(y_i - \hat{\mu}_{SRS})^2}{n(n-1)}, \tag{4b}$$

where i indexes the n sample units, and y_i is the observation for the ith sample unit. The primary advantages of the SRS estimators are that they are intuitive, simple, and unbiased when used with an SRS design; the disadvantage is that variances are frequently large, particularly for small sample sizes and/or populations with large variability among population unit observations. Although $V\hat{a}r(\hat{\mu}_{SRS})$ from Eq. (4b) may be biased when used with systematic sampling, it is usually conservative in the sense that it over-estimates the variance (Särndal et al., 1992). For this study, finite population correction factors were ignored because of the small sampling intensity of approximately one 168-m^2 plot per 3100 ha.

3.3.2. Model-assisted, generalized regression estimators

A *synthetic* estimator of the population mean is,

$$\hat{\mu}_{Syn} = \frac{1}{N}\sum_{i=1}^{N} \hat{y}_i, \tag{5a}$$

where N is the population size and $\hat{y}_i$ is the model AGB prediction for the ith population unit. Hansen et al. (1983) note that models that do not "represent the state of nature" induce bias into this estimator which, for equal probability samples, can be estimated as,

$$B\hat{i}as(\hat{\mu}_{Syn}) = \frac{1}{n}\sum_{i=1}^{n} \varepsilon_i, \tag{5b}$$

where $\varepsilon_i = \hat{y}_i - y_i$. The *model-assisted, generalized regression* (GREG) estimator is then defined as (Särndal et al., 1992; Särndal, 2011),

$$\begin{aligned}\hat{\mu}_{GREG} &= \hat{\mu}_{Syn} - B\hat{i}as(\hat{\mu}_{Syn}) \\ &= \frac{1}{N}\sum_{i=1}^{N}\hat{y}_i - \frac{1}{n}\sum_{i=1}^{n}\varepsilon_i.\end{aligned} \tag{5c}$$

When least squares techniques are used to estimate the model parameters, the bias estimate will be zero for linear models and is often small for nonlinear models (McRoberts et al., 2013). The corresponding GREG variance estimator is,

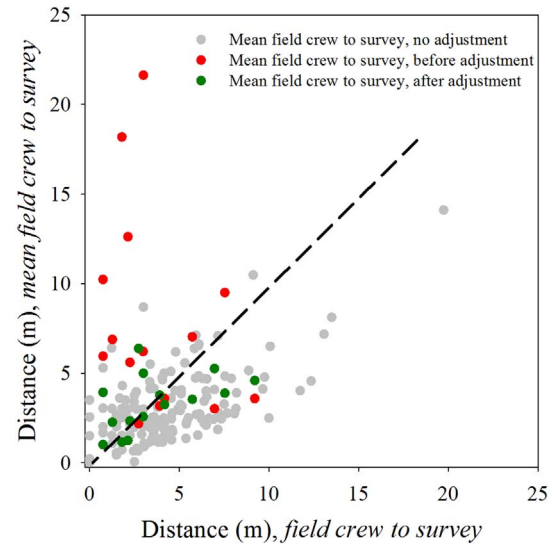

Fig. 2. The effects of adjusting mean field crew coordinates. Horizontal axis is distance from original field crew to survey coordinates; vertical axis is distance from original survey to mean field coordinates. Red and green data points represent the same plots, with mean coordinates before and after adjustment, respectively.

$$V\hat{a}r(\hat{\mu}_{GREG}) = \frac{1}{n(n-p)}\sum_{i=1}^{n}(\varepsilon_i - \bar{\varepsilon})^2, \tag{5d}$$

where p is the number of model parameters and $\bar{\varepsilon} = \frac{1}{n}\sum_{i=1}^{n}\varepsilon_i$ (Särndal et al., 1992; Särndal, 2011). The primary advantage of the GREG estimators is that they capitalize on the relationship between the sample observations and their model predictions to reduce the variance of the estimator of the population mean.

4. Results and discussion

4.1. Plot coordinates

Of the 242 FIA plots used for this study: (i) 46 non-forest plots had never been measured in field and, therefore, had no *survey* or *field crew* coordinates; (ii) 44 plots had only one or two sets of *field crew* coordinates; (iii) 145 plots had two or more sets of *field crew* coordinates, but required no adjustment of *mean field crew* coordinates, and (iv) 17 plots had two or more sets of *field crew* coordinates and required adjustment of the *mean field crew* coordinates. For *mean field crew* and/or *adjusted mean field crew* coordinates, the primary results were twofold (Fig. 2). First, the large proportion of data points falling below the 1:1 line indicates that *mean field crew* and *adjusted mean field crew* coordinates were generally closer to the *survey* coordinates than were the *field crew* coordinates. Second, for plots with three or more sets of *field crew* coordinates of which one deviated substantially from its respective mean (red data points), deleting the deviating *field crew* coordinates and recalculating the *mean field crew* coordinates brought the *adjusted mean field* crew coordinates (green points) much closer to the 1:1 line and, therefore, closer to the *field crew* and *survey* coordinates. Thus, the *mean field crew* and *adjusted mean field crew* coordinates were generally closer to the *survey* coordinates than were the original *field crew* coordinates.

4.2. Outliers

Three factors affected decisions as to whether plot observations should be considered outliers and deleted from the analyses. The first factor as described in Section 3.1 pertained to the disturbance of plots between ALS acquisition and field measurement. For the eight combinations of four kinds of plot coordinates and two response variables (AGB1, AGB5), 5–6 plots were deleted in consideration of this factor.

The effect of GPS location error on this factor was deletion of 1–2 additional plots as outliers. Because the effect was to delete more plots, albeit a small number, the original criterion based on h_{qm} for the plot location was used for all subsequent analyses. For the second factor, also described in Section 3.1 and pertaining to discrepancies between land use and land cover, 11–14 plots were deleted. The third factor as described in Section 3.2 related to large absolute values of standardized residuals. For this factor, 1–2 plots were deleted when using *survey* coordinates, whereas 3–5 plots were deleted when using the *field crew*-based coordinates. Overall, the less accurate *field crew*-based coordinates produced greater numbers of outliers for the first and third factors, but not for the second factor.

4.3. Model construction

For the eight combinations of kinds of plot coordinates and response variables, h_{qm} was the ALS metric that contributed most to statistically significantly improving the quality of fit of the models to the data. For models based on h_{qm}, R^{2*} ranged from 0.765 to 0.802 for AGB1 and from 0.776 to 0.864 for AGB5 with the greatest values, as expected, for the *survey* coordinates. Of importance, R^{2*} values obtained prior to deleting outliers as discussed in Section 4.2 were proportionally 0.19 to 0.29 smaller than R^{2*} values obtained after deleting outliers.

4.4. Inference

The overarching technical objective of the study was to estimate the degree to which use of ALS metrics corresponding to the *field crew*, *mean field crew*, and *adjusted mean field crew* coordinates induces bias into the GREG estimator of mean AGB per unit area and the degree to which uncertainty as expressed by the standard error of the mean is affected. For the nonlinear models used for this study, the effects of errors-in-variables on bias and precision are similar conceptually to regression dilution for linear models. If the bias is non-negligible and/or uncertainty is substantially increased, then operational use of ALS data for the inventory program would require purchasing expensive survey grade GPS receivers for all field crews. However, because the true mean is not known and only a single sample was available, a formal assessment of bias is not possible. Therefore, means and standard errors obtained for the *survey* coordinates were used as the standard for comparison.

The most important result was that estimates of mean AGB obtained using ALS metrics corresponding to *field crew*, *mean field crew*, and *adjusted mean field crew* coordinates deviated very little from estimates obtained using *survey* coordinates (Table 2). Estimates of mean AGB1 for the *field crew*-based coordinates deviated proportionally by no more than 0.01 from estimates for *survey* coordinates, and estimates for mean AGB5 deviated proportionally by no more than 0.04. Using only plot observations with no deletions and no auxiliary information, the SRS estimates of mean AGB for forest land use were $\hat{\mu}_{SRS} = 47.53$ Mg/ha with $SE(\hat{\mu}_{SRS}) = 3.91$ Mg/ha for AGB1 and $\hat{\mu}_{SRS} = 38.10$ Mg/ha with $SE(\hat{\mu}_{SRS}) = 3.72$ Mg/ha for AGB5. Because the ALS-assisted estimates for this study reflect AGB on all lands with tree cover, not just land with forest use, $\hat{\mu}_{SRS}$ should be expected to be less than $\hat{\mu}_{GREG}$. Nevertheless, $\hat{\mu}_{GREG}$ for all combinations of kinds of coordinates and response variables was always within two SRS SEs of $\hat{\mu}_{SRS}$.

Model prediction accuracy can be assessed not only via measures such as R^{2*} as per Eq. (3), but also via estimated bias as per Eq. (5b). The estimated biases were minimal, ranging from −0.36 to 0.60 Mg/ha or proportionally to means ranging from −0.01 to 0.02 (Table 2). These results suggest little is lost in terms of the accuracy of the population parameter estimate as expressed by estimated bias by using *field crew*, *mean field crew*, or *adjusted mean field crew* coordinates.

The expectation underlying the study was that the closer *field crew*-based plot coordinates are to the *survey* coordinates, the closer the estimates obtained using the *field crew*-based coordinates will be to the estimates obtained using the *survey* coordinates and the smaller the SEs will be. For estimated mean AGB1, differences between the SEs corresponding to the survey grade coordinates and the three sets of field crew coordinates were small, ranging from 0.06 to 0.20 Mg/ha. However, for the estimated mean AGB5, the differences were greater, ranging from 0.35 to 0.44 Mg/ha. No reason for the greater differences for the latter case is readily apparent. Although SEs for the three *field crew*-based coordinates were quite similar to each other, SEs for *adjusted mean field crew* coordinates were slightly greater than SEs for *mean field crew* coordinates which, in turn, were slightly greater than SEs for *field crew* coordinates. This result is difficult to explain given that the both the *mean field crew* and *adjusted mean field crew* coordinates were generally closer to the *survey* coordinates than the *field crew* coordinates (Section 4.1, Fig. 2). This result could, conceivably, be attributed to some combination of multiple factors. First, multiple instances were noted for which *adjusted mean field crew* coordinates were farther, rather than closer, to *survey* coordinates than *mean field crew* coordinates. This condition cannot be known, however, apart from acquisition of *survey* coordinates. Second, multiple instances were also noted for which differences in h_{qm} increased when differences between *mean field crew* and *survey* coordinates decreased. This phenomenon may be a consequence of forest fragmentation. Third, due to the nonlinear form of the model, equal positive and negative differences in h_{qm} do not necessarily result in equal differences in model predictions; similarly, equal differences in h_{qm} regardless of sign do not necessarily produce similar results for small and large predictions. Finally, the relatively small differences in SEs could be at least partially due simply to random effects.

4.5. Operational implications

From an operational perspective, multiple results merit emphasis. First, use of field grade GPS receivers with maximum locations errors of 5–10 m had effects of 5% or less on estimates of mean AGB per unit area. Second, the detrimental effects on standard errors of estimates of the means were greater, on the order of 5–20%. However, even the

Table 2
Estimates.

Minimum tree diameter at breast-height	Plot coordinates	R^{2*}	Mean aboveground biomass per unit area (Mg/ha)			
			$\hat{\mu}_{Syn}$	$\widehat{Bias}(\hat{\mu}_{Syn})$	$\hat{\mu}_{GREG}$	$SE(\hat{\mu}_{GREG})$
2.54 cm (1 in)	*Survey*	0.802	54.53	−0.36	54.89	1.84
	Field crew	0.796	54.78	0.08	54.70	1.90
	Mean field crew	0.777	54.83	0.00	54.83	1.99
	Adjusted mean field crew	0.765	55.26	0.25	55.01	2.04
12.70 cm (5 in)	*Survey*	0.864	42.60	−0.08	42.68	1.48
	Field crew	0.792	44.96	0.60	44.36	1.83
	Mean field crew	0.776	44.57	0.33	44.24	1.91
	Adjusted mean field crew	0.776	44.54	0.61	43.94	1.92

latter larger ALS-assisted standard errors were still substantially smaller than the satellite image-assisted standard errors currently reported by the inventory program for the study area (McRoberts et al., 2017). Third, the Northern Research Station of the U.S. Forest Service conducts the NFI in the region containing the study area and currently uses 110 field crews. Thus, the cost of acquiring an approximate $10,000 survey grade GPS receiver for each field crew would exceed $1 million. Further, because the Northern Research Station is just one of four Research Stations that conduct the inventory, the cost at the national level would be substantially greater. Thus, the primary operational finding was that circumventing the substantial additional cost of acquiring a survey grade GPS receiver for each of more than 100 field crews likely outweighs the adverse effects of the somewhat larger ALS-assisted standard errors corresponding to field grade GPS receivers that those corresponding to survey grade receivers.

5. Conclusions

Three conclusions were drawn from the study. First, the results benefitted considerably from deletion of observations for two kinds of plots: (i) plots experiencing substantial disturbance between the dates of airborne laser scanning data acquisition and plot measurement and (ii) plots characterized as non-forest use but with substantial tree cover. Second, although *mean field crew* and *adjusted mean field crew* coordinates were generally closer to the *survey* coordinates than the *field crew* coordinates, standard errors based on the former coordinates were slightly larger than standard errors based on the *field crew* coordinates. Nevertheless, as more sets of *field crew* coordinates are obtained using more accurate GPS receivers, consideration of *mean field crew* and *adjusted mean field crew* coordinates should continue. Third, and most importantly for inventory applications, estimates of mean aboveground biomass per unit area obtained using *field crew*, *mean field crew*, and *adjusted mean field crew* coordinates did not deviate substantially from estimates obtained using *survey* coordinates. In particular, differences were proportionally less than 0.01 for biomass in trees with diameters of at least 2.54 cm (1 in) and less than 0.04 for biomass in trees with diameters of at least 12.70 cm (5 in). In addition, although the *field crew*, *mean field crew*, and *adjusted mean field crew* coordinates caused standard errors to increase, the differences were not compelling. From an operational perspective, these slightly larger standard errors may be an acceptable compromise if the alternative is purchasing very expensive survey grade GPS receivers for all field crews.

Acknowledgements

The authors thank Mr. Richard McCullough, Northern Research Station, U.S. Forest Service, Newtown Square, PA, for assisting in documenting the specifications for the GPS receivers.

References

Babcock, C., Finley, A.O., Bradford, J.B., Birdsey, R., Ryan, M.G., 2015. LiDAR based prediction of forest biomass using hierarchical models with spatially varying coefficients. Remote Sens. Environ. 169, 113–127.
Bickford, C.A., 1952. The sampling design used in the forest survey of the northeast. J. For. 50, 290–293.
Boudreau, J., Nelson, R.F., Margolis, H.A., Beaudoin, A., Guindon, L., Kimes, D.S., 2008. Regional aboveground forest biomass using airborne and spaceborne LiDAR in Quebec. Remote Sens. Environ. 112, 3876–3890.
Cao, L., Coops, N.C., Innes, J.L., Sheppard, S.R.J., Fu, L., Ruan, H., She, G., 2016. Estimation of forest biomass dynamics in subtropical forests using multi-temporal airborne LiDAR data. Remote Sens. Environ. 178, 158–171.
Chen, Q., 2007. Airborne lidar data processing and information extraction. Photogramm. Eng. Remote. Sens. 73 (12), 1355–1365.
Chen, Q., 2015. Modeling aboveground tree woody biomass using national-scale allometric methods and airborne lidar. ISPRS J. Photogramm. Remote Sens. 106, 95–106.
Chen, Q., Vaglio Laurin, G., Battles, J.J., Saah, D., 2012. Integration of airborne lidar and vegetation types derived from aerial photography for mapping aboveground live biomass. Remote Sens. Environ. 121, 108–117.
Chen, Q., McRoberts, R.E., Wang, C., Radtke, P.J., 2016. Forest aboveground biomass mapping and estimation across multiple spatial scales using model-based inference. Remote Sens. Environ. 184, 350–360.
Chirici, G., McRoberts, R.E., Fattorini, L., Mura, M., Marchetti, M., 2016. Comparing echo-based and canopy height model-based metrics for enhancing estimation of forest aboveground biomass in a model-assisted framework. Remote Sens. Environ. 174, 1–9.
Draper, N.R., Smith, H., 1981. Applied Regression Analysis, 2nd ed. Wiley.
FAO, 2016. Global Forest Resources Assessment, 2015. Food and Agriculture Organization of the United Nations, Rome 47 pp. Available at: http://www.fao.org/3/a-i4793e.pdf, Accessed date: July 2016.
Frazer, G.W., Magnussen, S., Wulder, M.A., Niemann, K.O., 2011. Simulated impact of sample plot size and co-registration error on the accuracy and uncertainty of LiDAR-derived estimates of forest stand biomass. Remote Sens. Environ. 115, 636–649.
Gobakken, T., Næsset, E., 2008. Assessing effects of laser point density, ground sampling intensity, and field plot sample size on biophysical stand properties derived from airborne laser scanner data. Can. J. For. Res. 38, 1095–1109.
Gobakken, T., Næsset, E., 2009. Assessing effects of positioning errors and sample plot size on biophysical stand properties derived from airborne laser scanner data. Can. J. For. Res. 39, 1036–1052.
Hansen, M.H., Madow, W.G., Tepping, B.J., 1983. An evaluation of model dependent and probability-sampling inferences in sample surveys. J. Am. Stat. Assoc. 78, 776–793.
Hollaus, M., Dorigo, W., Wagner, Schadauer, K., Höfle, B., Maier, B., 2009. Operational wide-area stem volume estimation based on airborne laser scanning and national forest inventory data. Int. J. Remote Sens. 30 (19), 5159–5175.
Hopkinson, C., Chasmer, L., Barr, A.G., Kljun, N., Black, T.A., McCaughey, J.H., 2016. Monitoring boreal forest biomass and carbon storage change by integrating airborne laser scanning, biometry and eddy covariance data. Remote Sens. Environ. 181, 82–95.
Lefsky, M.A., Harding, D., Cohen, W.B., Parker, G., Shugart, H.H., 1999. Surface lidar remote sensing of basal area and biomass in deciduous forests of eastern Maryland, USA. Remote Sens. Environ. 67, 83–98.
Magnussen, S., Boudewyn, P., 1998. Derivations of stand heights from airborne laser scanning data with canopy-based quantile estimators. Can. J. For. Res. 28, 1016–1031.
Mauro, F., Valbuena, R., Manznaera, J.A., Garcia-Abril, A., 2011. Influence of Global Navigation Satellite System errors in positioning inventory plots for tree height distribution studies. Can. J. For. Res. 41, 11–23.
McRoberts, R.E., Wendt, D.G., Nelson, M.D., Hansen, M.D., 2002. Using a land cover classification based on satellite imagery to improve the precision of forest inventory area estimates. Remote Sens. Environ. 81, 36–44.
McRoberts, R.E., Holden, G.R., Nelson, M.D., Liknes, G.C., Gormanson, D.D., 2006. Using satellite imagery as ancillary data for increasing the precision of estimates for the Forest Inventory and Analysis program of the USDA Forest Service. Can. J. For. Res. 36, 2968–2980.
McRoberts, R.E., Hansen, M.H., Smith, W.B., 2010. United States of America. In: Tomppo, E., Gschwantner, T., Lawrence, M., McRoberts, R.E. (Eds.), National Forest Inventories, Pathways for Common Reporting. Springer.
McRoberts, R.E., Gobakken, T., Næsset, E., 2012. Post-stratified estimation of forest area and growing stock volume using lidar-based stratifications. Remote Sens. Environ. 125, 157–166.
McRoberts, R.E., Næsset, E., Gobakken, T., 2013. Inference for lidar-assisted estimation of forest growing stock volume. Remote Sens. Environ. 128, 268–275.
McRoberts, R.E., Chen, Q., Domke, G.M., Ståhl, G., Saarela, S., Westfall, J.A., 2016. Hybrid estimators for mean aboveground carbon per unit area. For. Ecol. Manag. 378, 44–56.
McRoberts, R.E., Chen, Q., Walters, B.F., 2017. Multivariate inference for forest inventories using auxiliary airborne laser scanning data. For. Ecol. Manag. 401, 295–303.
Miles, P.D., Heinzen, D., Mielke, M.E., Woodall, C.W., Butler, B.J., Piva, R.J., Meneguzzo, D.M., Perry, C.H., Gormanson, D.D., Barnett, C.J., 2011. Minnesota's forests 2008. In: Resource Bulletin NRS-50. U.S. Department of Agriculture, Forest Service, Northern Research Station, Newtown Square, PA.
Næsset, E., Gobakken, T., Solberg, S., Gregoire, T.G., Nelson, R., Ståhl, G., Weydahl, D., 2011. Model-assisted regional forest biomass estimation using LiDAR and InSAR as auxiliary data: a case study from a boreal forest area. Remote Sens. Environ. 115, 3599–3614.
Nelson, R., Boudreau, R., Gregoire, T.G., Margolis, H., Naesset, E., Gobakken, T., Stahl, G., 2009. Estimating quebec provincial forest resources using ICESat/GLAS. Can. J. For. Res. 39, 862–881.
Nilsson, M., Holm, S., Reese, H., Wallerman, J., Engberg, J., 2005. Improved forest statistics from the Swedish National Forest Inventory by combining field data and optical satellite data using post-stratification. In: Olsson, H. (Ed.), Proceedings of ForestSat 2005, Bora˚s, Sweden, May 31–June 3, 2005. National Board of Forestry, Sweden, Jönköping, pp. 22–26.
Nilsson, M., Nordkvist, K., Jonzén, J., Lindgren, N., Axensten, P., Wallerman, J., Egberth, M., Larsson, S., Nilsson, L., Olsson, H., 2017. A nationwide forest attribute map of Sweden predicted using airborne laser scanning data and field data from the National Forest Inventory. Remote Sens. Environ. 194, 447–454.
Poso, S., 1972. A method for combining photo and field samples in forest inventory. Commun. Inst. For. Fenniae 76, 1–133.
Poso, S., Kujala, M., 1978. A method for national forest inventory in northern Finland. Commun. Inst. For. Fenniae 93, 1–54.
Saarela, S., Grafström, A., Ståhl, G., Kangas, Holopainen, M., Tuominen, S., Nordkvist, K., Hyyppä, J., 2015. Model-assisted estimation of growing stock volume using different combinations of LiDAR and Landsat data as auxiliary information. Remote Sens. Environ. 158, 431–440.

Saarela, S., Schnell, S., Tuominen, S., Balázs, A., Hyppä, J., Grafström, A., Ståhl, G., 2016. Effects of positional errors in model-assisted and model-based estimation of growing stock volume. Remote Sens. Environ. 172, 101–108.
Särndal, C.-E., 2011. Combined inference in survey sampling. Pak. J. Stat. 27, 359–370.
Särndal, C.-E., Swensson, B., Wretman, J., 1992. Model Assisted Survey Sampling. Springer-Verlag, Inc.
Steinmann, K., Mandallaz, D., Ginzler, C., Lanz, A., 2013. Small area estimations of proportion of forest and timber volume combining Lidar data and stereo aerial images with terrestrial data. Scand. J. For. Res. 28 (4), 373–385.
UNFCCC, 2006. Updated UNFCCC Reporting Guidelines on Annual Inventories Following Incorporation of the Provisions of Decision 14/CP.11. Note by the Secretariat. United Nations Office at Geneva, Geneva, Switzerland (93 pp.).
USDA Forest Service (USDA-FS), 2012. Future of America's Forest and Rangelands: Forest Service 2010 Resources Planning Act Assessment. General Technical Report WO-87. (Washington, DC).
Vauhkonen, J., Maltamo, J., McRoberts, R.E., Næsset, E., 2014. Introduction to forestry applications of airborne laser scanning data. In: Maltamo, M., Næsset, E., Vauhkonen, J. (Eds.), Forestry Applications of Airborne Laser Scanning. Springer, Dordrecht, pp. 1–16.